

## Influence of the Northern Hemisphere annular mode on ENSO by modulating westerly wind bursts

Tetsu Nakamura,<sup>1</sup> Yoshihiro Tachibana,<sup>1,2</sup> Meiji Honda,<sup>3</sup> and Shozo Yamane<sup>3,4</sup>

Received 8 December 2005; revised 31 January 2006; accepted 20 February 2006; published 5 April 2006.

[1] The influence of the Northern Hemisphere annular mode (NAM) on the El Niño/Southern Oscillation (ENSO) was examined using 41-year reanalysis data and an atmospheric general circulation model (AGCM). Significant lag correlations between the NAM index for spring and the Niño-3 index for the following winter were revealed. An anomalous lower tropospheric westerly associated with modulation of the westerly wind burst (WWB) over the western tropical Pacific in spring often coincided with the positive phase of the NAM and extended eastward during summer and autumn. Then, warm sea surface temperature (SST) anomalies reflecting El Niño appeared over the eastern tropical Pacific in early winter. In an AGCM experiment in which SSTs were fixed as a climatological-mean monthly distribution, the interannual modulation of WWB was significantly associated with NAM variability in spring, supporting the possible influence of the NAM in spring on an ENSO outbreak the following winter. **Citation:** Nakamura, T., Y. Tachibana, M. Honda, and S. Yamane (2006), Influence of the Northern Hemisphere annular mode on ENSO by modulating westerly wind bursts, *Geophys. Res. Lett.*, 33, L07709, doi:10.1029/2005GL025432.

### 1. Introduction

[2] The El Niño/Southern Oscillation (ENSO) and Northern Hemisphere Annular Mode or Arctic Oscillation (NAM hereafter) are the major active factors in the climate variability at midlatitudes. For example, the ENSO might excite the Pacific/North American pattern at midlatitudes [Wallace and Gutzler, 1981; Horel and Wallace, 1981]. The NAM influences wintertime climate, especially over Eurasia [Thompson and Wallace, 1998; Xie et al., 1999; Ogi et al., 2004b]. Numerous studies have examined the effects of the NAM and ENSO. However, these studies have generally been conducted separately, and the direct relationships between the NAM and ENSO require further clarification. Further, few studies have examined the influence of the NAM on the tropics. Recently, Zhou and Miller [2005] revealed Madden-Julian oscillation (MJO) influences on the NAM, but their focus was on the tropical influences on mid-

and high latitudes. Conversely, Thompson and Lorenz [2004] attempted to detect the effects of both hemispheric annular modes (AMs) on the tropics. They showed coupling between the AMs and tropical atmosphere and that a wintertime positive (negative) AM generates the upper tropospheric zonal mean westerly (easterly) anomalies in the tropics after a 2-week lag. These results suggest a link between the NAM and tropical variability. However, they did not note any direct influences of the NAM on the ENSO.

[3] This study examined the influences of NAM on the ENSO. Based on the results of previous studies, we examined the lead and lag relationships between the NAM and ENSO in all seasons using a reanalysis data set. The observational evidence revealed a statistically significant relationship between the NAM signature and the ENSO. To strengthen this finding, we also used an atmospheric general circulation model (AGCM) to simulate climatological monthly mean sea surface temperature (SST) distributions.

### 2. Data and Indices

[4] The National Centers for Environmental Prediction/National Center for Atmospheric Research (NCEP/NCAR) reanalysis [Kalnay et al., 1996] monthly mean data for 45 years (1958–2002) were used in this study. The ocean data set included the global monthly sea ice coverage and SST data (GISST2.3b) measured by the United Kingdom Meteorological Office from 1958 to 2000. All the data were averaged for two successive months before use to remove the MJO time scale, which may affect the NAM [Zhou and Miller, 2005]. The NAM index was defined as by Ogi et al. [2004a], except for the use of the 2-month mean field. The spring (March and April mean in this study) NAM pattern was similar to the original Arctic Oscillation pattern [Thompson and Wallace, 1998, 2000] (not shown). The monthly mean Niño-3 index, which is the area-averaged SST between 5°S–5°N and 150°W–90°W from 1958 to 2003 (provided by Climate Prediction Center), was used as an indicator of ENSO events. The Niño-3 index was also averaged for every two months.

[5] The original atmospheric and oceanic data sets generally included multiple time scales, including trends and interdecadal variation. To isolate ENSO-related variability, which has roughly a 4-year time scale, we applied a high-pass filter to all the original data and indices; the filter subtracted 5-year moving averages from the original values. The results in this study did not heavily depend on the type of high-pass filter (i.e., subtracting 2-, 3-, or 4-year moving average). Our analysis is primarily based on simultaneous and lead-lag linear regression and correlation methods. The 1-year lagged autocorrelation coefficients of the high-pass

<sup>1</sup>Graduate School of Earth and Environmental Science, Tokai University, Hiratsuka, Japan.

<sup>2</sup>Institute of Observational Research for Global Change, Japan Agency for Marine-Earth Science and Technology Center, Yokosuka, Japan.

<sup>3</sup>Frontier Research Center for Global Change, Japan Agency for Marine-Earth Science and Technology Center, Yokohama, Japan.

<sup>4</sup>Faculty of Risk and Crisis Management, Chiba Institute of Science, Choshi, Japan.

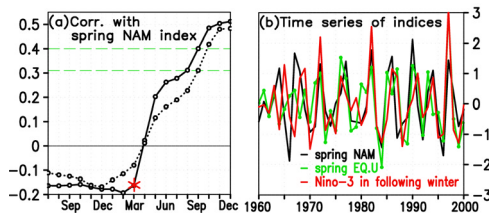


**Figure 1.** (a) Seasonal evolution of the correlation coefficients (solid line) and covariance value [°C] (dotted line) between the Niño-3 index from July in the previous year to the following December and the NAM index in spring (March–April mean) based on 45-year NCEP-NCAR reanalysis data. Since this study used 2-month means, March, for example, indicates the mean value for March and April. Trends and low-frequency variation were removed from both indices (see text for details). The green and dashed lines show the 95 and 99% significant levels, respectively. A red star indicates the time of the simultaneous correlation in spring. (b) Time series of the NAM index and equatorial zonal wind (150°E, 850-hPa) in spring and the Niño-3 index in the following winter (averaged for December and January in the following year) from 1960 to 2000. All the indices are standardized.

filtered indices were less than 0.3, indicating that the interactive contribution between the two time series was less than 10%. Therefore, we could regard both indices as independent, with 37 degrees of freedom for the correlation for the GISST data and 39 degrees of freedom for the other data. Because we use 2-month mean field, we should notice the statistical significances in this study. Each 2-month period could be regarded as independent, allowing for six possible changes of correlation in one year. Therefore, the chance of more than one change in correlation was approximately 26% ( $= 1 - 0.95^6$ ) at the 95% confidence level and 6% ( $= 1 - 0.99^6$ ) at the 99% level. In climate studies, a risk of 6% has adequate validity. Therefore, we focused on whether the correlations

were over the 99% level in the following sections. Results calculated using the calendar-month means did not change substantially. Note that the sign of the linear regression maps in the following sections always corresponds to the positive phase of the NAM in this study.

### 3. Observational Evidence

[6] Figure 1a shows the lead-lag correlation coefficients between the NAM index in spring and the Niño-3 index from the previous July to the following December. The correlation coefficients are nearly zero or slightly negative on the left-hand side of Figure 1a, where the NAM lags behind Niño-3. The simultaneous correlations are still nearly zero. By contrast, the correlation jumps to a positive value in late spring, gradually increases in summer, and exceeds the 99% significant level from July to December. This indicates that warm SST anomalies in the eastern tropical Pacific tend to appear in the winter following a positive springtime NAM. No such a significant lag correlation was found for the other months of the NAM index. The time series of the spring NAM index and Niño-3 index in the following winter were also similar (Figure 1b). This indicates that the significant correlation was not due to one or two extreme events.

[7] A westerly wind burst over the western tropical Pacific is known to trigger El Niño outbreaks [e.g., Luther *et al.*, 1983; Barnett, 1983; Barnett *et al.*, 1989]. Therefore, we focused on the NAM contribution to the region of WWBs. Figure 2a shows the simultaneous regression coefficients between the NAM index and the zonal wind anomalies over the Equator in spring. The positive center of the regression coefficients, that is, the westerly wind anomalies associated with the NAM, appeared around 150°E in the lower troposphere. We also examined tropical horizontal wind patterns regressed linearly onto the spring NAM. In the lower troposphere, the horizontal pattern of the tropical wind anomaly associated with the positive NAM appeared to have a twin vortex structure over the western tropical Pacific (not shown). The NAM-related anomalous

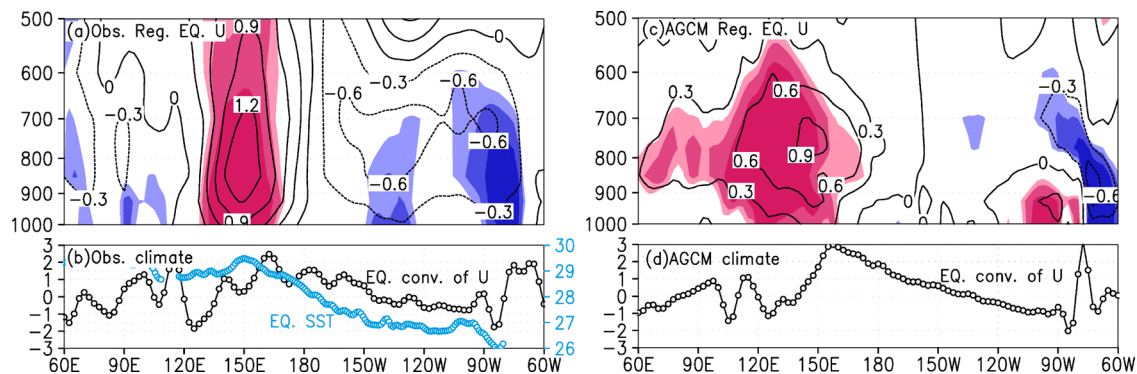


**Figure 2.** (a) Linear regression coefficients between the zonal wind anomalies over the Equator and the NAM index in spring (March–April mean) based on the 45-year NCEP-NCAR reanalysis. The trends and low-frequency variation of all fields were removed in advance. Contours correspond to a local change in velocities when the NAM increases by its unit standard deviation. Contour intervals are 0.3 [ms<sup>-1</sup>] and red (blue) shading indicates positive (negative) correlations. Light, moderate, and heavy shadings indicate significant at 90, 95, and 99% confidence levels, respectively. (b) The climatological mean SST (blue) and vertical averaged (from 1000–700 hPa) convergence of the zonal wind (black; positive values correspond to convergence) over the Equator in spring based on the GISST2.3b data set and NCEP-NCAR reanalysis data. The horizontal axis represents longitude [deg.]. The vertical axes ranged from 26 to 30 [°C] for SST and from  $-3 \times 10^{-6}$  to  $3 \times 10^{-6}$  [s<sup>-1</sup>] for convergence. (c, d) As in Figures 2a and 2b, except based on the AGCM-simulated 45-year data set.

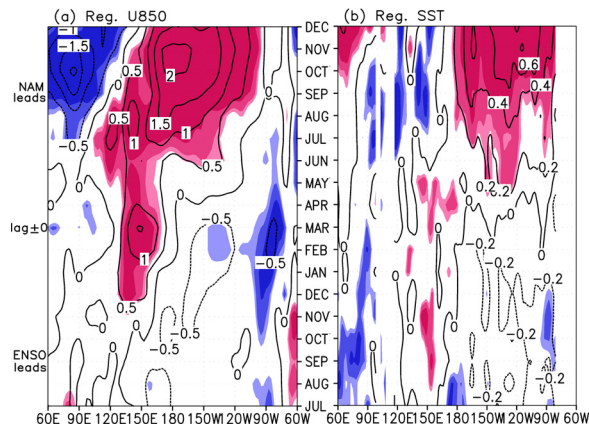


**Figure 3.** Seasonal evolution of the linear lag regression coefficients of the observational (a) equatorial zonal wind at 850-hPa [ $\text{ms}^{-1}$ ] and (b) equatorial SST [ $^{\circ}\text{C}$ ] from July in the previous year to the following December and the NAM index in spring (March–April mean). The contours correspond to a local change in height (Figure 3a) and SST (Figure 3b) when the spring NAM index increases by its unit standard deviation. The trends and low-frequency variation of all fields were removed in advance. Red (blue) shading indicates westerly (easterly) (Figure 3a) and warm (cold) (Figure 3b). The contour interval is 0.5 [ $\text{ms}^{-1}$ ] in Figure 3a and 0.2 [ $^{\circ}\text{C}$ ] in Figure 3b. Light, moderate, and dark shading indicates that the correlation between zonal wind (Figure 3a) or SST (Figure 3b) over the Equator and the NAM index in spring was significant at the 90, 95, and 99% confidence levels, respectively.

westerlies blew between the two vortices. The area of NAM-related westerlies was just over the climatological SST maximum area (Figure 2b), which corresponds to the convection center caused by active atmosphere-ocean interactions [e.g., Wang, 1992] and the convergence zone of the climatological zonal wind in the equatorial lower atmosphere (positive values correspond to convergence in Figure 2b). This condition indicates that the anomalous westerly wind area broadened over the warm SST pool when the NAM was in the positive phase in spring, which satisfies a necessary condition for an El Niño outbreak as presented by Barnett *et al.* [1989].

[8] The temporal evolution of the equatorial zonal wind in relation to the NAM was also examined. Figures 3a and 3b show the lead and lag regression coefficients, respectively, (from the previous July to the following December) of the zonal wind at 850-hPa and the SST over the Equator on the NAM index in spring. When the NAM was positive in spring, an anomalous westerly was simultaneously evident over the western equatorial Pacific (Figure 3a). This westerly anomaly was maintained throughout the summer before then broadening toward the eastern tropical Pacific in autumn. In the following early winter, the significant westerly anomaly eventually covered most of the western Pacific. Similar tendencies were seen at other levels of the lower troposphere (not shown). Although the lag correlations of the SST and the NAM index in spring revealed no significant signatures from spring to summer (Figure 3b), warm SST anomalies gradually appeared in autumn, and significant warm anomalies

corresponding to an El Niño event become evident in winter. These lag-correlated tendencies of the spring NAM substantially follow the typical evolution of El Niño development. While significant lagged tropical signatures associated with the spring NAM are evident, no clear signals could be found in the former seasons. These results also suggest that the spring NAM is not a response to ENSO, but rather that the NAM or its associated phenomena act to trigger ENSO in the following winter.

[9] Observational evidence based on the reanalysis data show that the NAM activates the ENSO. However, SST variations in the Niño-3 or other ocean regions in spring may influence both the spring NAM and WWB. Influence of a third factor on the WWB and NAM may cause their significant correlation. The tropical Indian Ocean SST is one strong possibility for such a third factor [e.g., Kawamura *et al.*, 2001; Wu and Kirtman, 2004; Annamalai *et al.*, 2005]. However, analysis using the partial correlation method, by which linearly correlated fields and indices with the tropical Indian SST were removed by linear regression, also showed substantially similar results to those presented above. This indicates that the connection between the NAM and WWB is still present without the influence of SST anomalies in the Indian Ocean. Another partial correlation in which the influence of Niño-3 SST was linearly removed also did not change the significant correlation between the NAM and WWB. These results indicate that the present findings do not merely demonstrate the influence of the tropics on the midlatitudes.

[10] However, evidence from observational data analyses alone may not completely clarify whether the NAM is a cause or a result. To confirm the causal relationship, we investigated the behaviors of wind anomalies associated with the NAM over the western equatorial Pacific using simulated atmospheric fields produced by an AGCM experiment without interannual variation in SST.

#### 4. Model Evidence

[11] This study used an AGCM for the Earth Simulator (AFES) [Ohfuchi *et al.*, 2004] that had triangular truncation at wave number 42 and 20 vertical levels (T42L20). To exclude the influence of interannual SST variability, we fixed the SSTs as observed climatological monthly mean values. Therefore, the atmospheric fields in this AGCM, by definition, included the influence of neither ENSO nor the Indian Ocean; this situation is generally referred to as a “control run”. We performed the control run for 60 years using the climatological SST and sea-ice conditions. Data from the first 15-year run were not used in this study because it takes several years for the simulation to spin up and stabilize. Therefore, we used the final 45 years of data. As for the observation data, all the data from the AGCM output were averaged for every 2 months. A 5-year high-pass filter, as used for the observational data, was also applied to the AGCM fields because long-term internal atmospheric variability (e.g., at a decadal time scale) generally appeared in model outputs, even in the ideal experiment with fixed SST.

[12] The simulated climatological mean zonal convergence over the Equator in spring (Figure 2d) agreed well with the observations shown in Figure 2b, so this model

successfully reproduces the tropic situations. The AGCM NAM index was defined as by Ogi *et al.* [2004a], except for the use of the 2-month mean model field. The spatial geopotential height patterns of the leading mode in spring essentially reproduced the observational NAM patterns (not shown).

[13] The simultaneous regression patterns of the zonal wind anomalies with the AGCM NAM index in spring (Figure 2c) were also highly similar to those from the observational data (Figure 2a). The center of the anomalous westerly associated with the AGCM NAM was located just over the climatological zonal convergence zone. These results show that when the NAM in spring is in a positive phase, westerly wind tends to blow over the western equatorial Pacific. The twin vortex structure associated with the NAM was also seen over the tropical Pacific in the model simulations (not shown). These model-simulated NAM signatures in the tropics are quite consistent with the observed signatures. The agreement between the model and observational results supports the observational evidence that atmospheric variation associated with the NAM can trigger the ENSO.

## 5. Summary and Possible Mechanisms

[14] Using both the observational and model-simulated evidence, we have shown that the NAM can influence the ENSO by exciting a zonal wind anomaly in the western tropical Pacific. The study results showed that El Niño (La Niña) tends to occur at the beginning of winter, preceded by an anomalous westerly (easterly) over the equatorial Pacific that has persisted since the previous spring in association with a positive (negative) NAM phase in spring. Similar results obtained from an AGCM experiment with fixed monthly SST strongly support the observational evidence. Future studies should investigate explanations for the physical linkage between the NAM and WWBs. It is possible that the horizontal pattern of the tropical wind anomaly associated with the spring NAM has a twin-vortex-like structure. This structure, which is similar to the equatorial Rossby response when the atmosphere gains heat, induces the westerly winds [Matsuno, 1966]. The positive NAM indicates a strong polar jet. The associated zonal mean meridional circulation, which features anomalous ascent at high latitudes and anomalous subsidence at midlatitudes, occurs from dynamic requirements [Limpasuvan and Hartmann, 2000]. Subsidence in the midlatitudes should strengthen the midlatitude side of the Hadley cell, indicating that anomalous northerlies from the midlatitudes to the tropics tend to blow in the lower atmosphere. A strong meridional gradient of temperature and moisture between the Asian continent and tropical warmest SST pool exists because this area faces both the warmest SST region to the south and the quite cold and dry continent to the north. The anomalous northerlies caused by the strengthening of the Hadley cell would bring strong, cold, and dry advections from the Asian continent to the equatorial western Pacific. The cold and dry air reaching the tropics would receive relatively large sensible and latent

heat from warm SSTs, especially at the warm SST pool. These processes may induce the twin-vortex structure and associated westerlies. This issue will be pursued further in future research.

[15] **Acknowledgments.** We wish to convey our thanks to K. Takaya, K. Kodera and K. Yamazaki for their helpful suggestions. Suggestions from anonymous reviewers are also helpful. The Grid Analysis and Display System (GrADS) was used for drawing figures.

## References

- Annamalai, H., S. P. Xie, J. P. McCreary, and R. Murtugudde (2005), Impact of Indian Ocean sea surface temperature on developing El Niño, *J. Clim.*, *18*, 302–319.
- Barnett, T. P. (1983), Interaction of the monsoon and Pacific trade wind system at inter-annual time scales. Part I: The equatorial zone, *Mon. Weather Rev.*, *111*, 756–773.
- Barnett, T., P. L. Dümenil, U. Schlese, E. Roeckner, and M. Latif (1989), The effect of Eurasian snow cover on regional and global climate variations, *J. Atmos. Sci.*, *46*, 661–686.
- Horel, J. D., and J. M. Wallace (1981), Planetary-scale atmospheric phenomena associated with the southern oscillation, *Mon. Weather Rev.*, *109*, 813–829.
- Kalnay, E., et al. (1996), The NCEP/NCAR 40-year reanalysis project, *Bull. Am. Meteorol. Soc.*, *77*, 437–471.
- Kawamura, R., T. Matsuura, and S. Iizuka (2001), Role of equatorially asymmetric sea surface temperature anomalies in the Indian Ocean in the Asian summer monsoon and El Niño–Southern Oscillation coupling, *J. Geophys. Res.*, *106*, 4681–4694.
- Limpasuvan, V., and D. L. Hartmann (2000), Wave-maintained annular modes of climate variability, *J. Clim.*, *13*, 4414–4429.
- Luther, D., D. Harrison, and R. Knox (1983), Zonal wind in the central equatorial Pacific and El Niño, *Science*, *202*, 327–330.
- Matsuno, T. (1966), Quasi-geostrophic motions in the equatorial area, *J. Meteorol. Soc. Jpn.*, *44*, 25–43.
- Ohfuchi, W., et al. (2004), 10-km mesh meso-scale resolving simulations of the global atmosphere on the Earth simulator—Preliminary outcomes of AFES (AGCM for the Earth simulator), *J. Earth Simulator*, *1*, 8–34.
- Ogi, M., K. Yamazaki, and Y. Tachibana (2004a), Summertime annular mode in the Northern Hemisphere and its linkage to the winter mode, *J. Geophys. Res.*, *109*, D20114, doi:10.1029/2004JD004514.
- Ogi, M., Y. Tachibana, and K. Yamazaki (2004b), The connectivity of the winter North Atlantic Oscillation (NAO) and the summer Okhotsk high, *J. Meteorol. Soc. Jpn.*, *82*, 905–913.
- Thompson, D. W. J., and D. J. Lorenz (2004), The signature of the annular modes in the tropical troposphere, *J. Clim.*, *17*, 4330–4342.
- Thompson, D. W. J., and J. M. Wallace (1998), The Arctic Oscillation signature in the wintertime geopotential height and temperature fields, *Geophys. Res. Lett.*, *25*, 1297–1300.
- Thompson, D. W. J., and J. M. Wallace (2000), Annular modes in the extratropical circulation. part I: Month-to-month variability, *J. Clim.*, *13*, 1000–1016.
- Wallace, J. M., and D. S. Gutzler (1981), Teleconnections in the geopotential height field during the Northern Hemisphere winter, *Mon. Weather Rev.*, *109*, 784–812.
- Wang, B. (1992), The vertical structure and development of the ENSO anomaly mode during 1979–1989, *J. Atmos. Sci.*, *49*, 698–712.
- Wu, R., and B. P. Kirtman (2004), Impacts of the Indian Ocean on the Indian summer monsoon–ENSO relationship, *J. Clim.*, *17*, 3037–3054.
- Xie, S.-P., H. Noguchi, and S. Matsumura (1999), A hemispheric-scale quasi-decadal oscillation and its signature in northern Japan, *J. Meteorol. Soc. Jpn.*, *77*, 573–582.
- Zhou, S., and A. J. Miller (2005), The interaction of the Madden-Julian Oscillation and the Arctic Oscillation, *J. Clim.*, *18*, 143–159.

M. Honda and S. Yamane, Frontier Research Center for Global Change, Japan Agency for Marine–Earth Science and Technology Center, 3173-25 Showamachi, Kanazawa-ku, Yokohama, Kanagawa 236-0001, Japan. (meiji@jamstec.go.jp; syamane@cis.ac.jp)

T. Nakamura and Y. Tachibana, Graduate School of Earth and Environmental Science, Tokai University, 1117 Kitakaname, Hiratsuka, Kanagawa 259-1292, Japan. (tetsu@rh.u-tokai.ac.jp; tachi@rh.u-tokai.ac.jp)